Study on the initial position of Taylor vortex for Taylor-Couette-Poiseuille flow formed by supercritical carbon dioxide

Fengxiong Lu, IET, UCAS

Chaohong Guo*, IET, UCAS

Shijie Zhang, IET, UCAS

Buze Chen, IET, UCAS

Bo Wang, IET, UCAS

Xiang Xu, IET, UCAS

INTRODUCTION

◆**Supercritical carbon dioxide Brayton cycle**

— Compactness

— Rapid response

— High power generation efficiency

— Flexibility

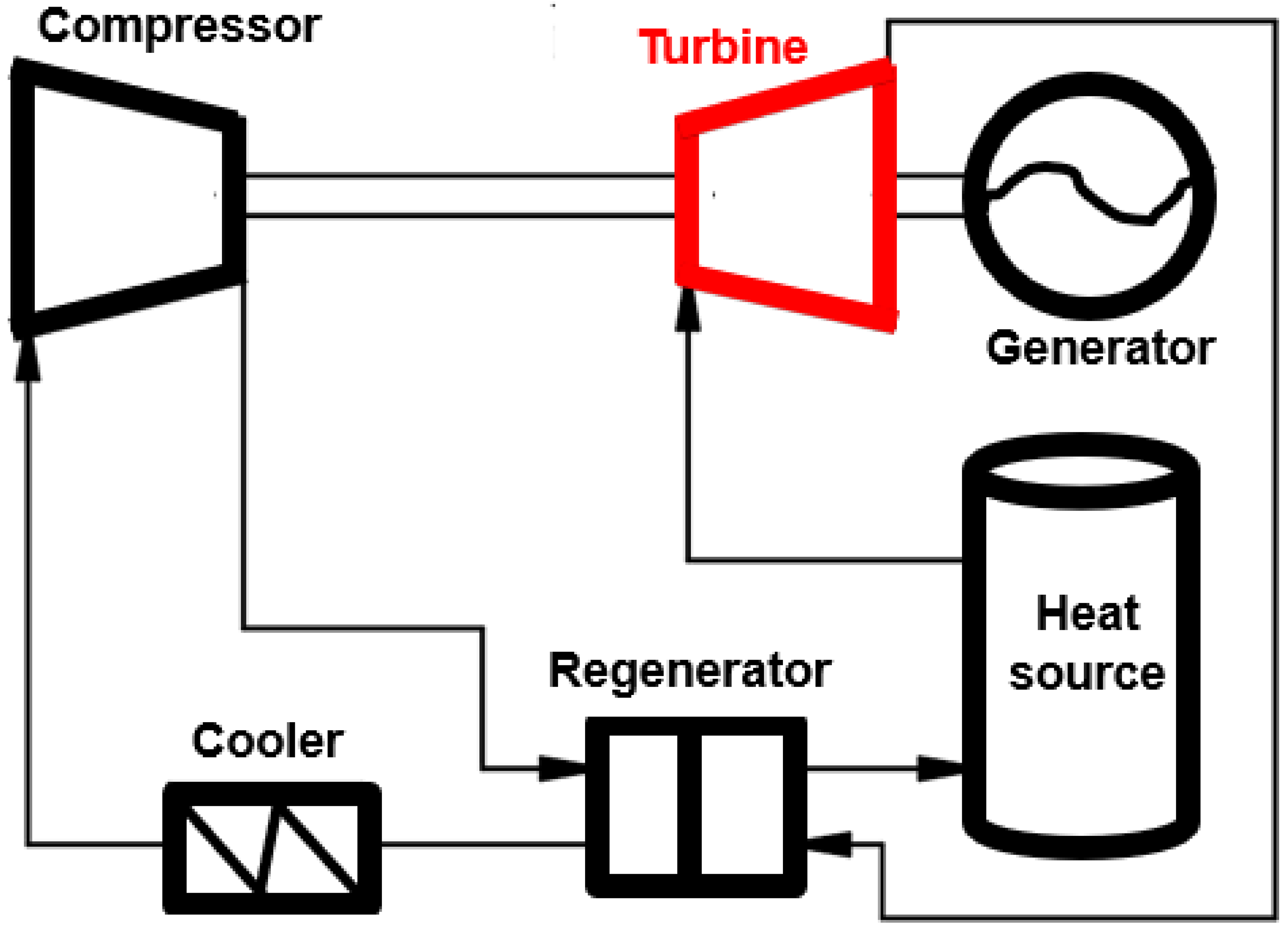

◆**Turbine is one of the key equipment**

— High temperature \ Pressure \ Rotational speed

◆**Achieving effective cooling**

—From the high temperature end (>500℃) to the low-temperature end of the bearing (<150℃) within a confined space

— Utilizing the sCO_2 fluid

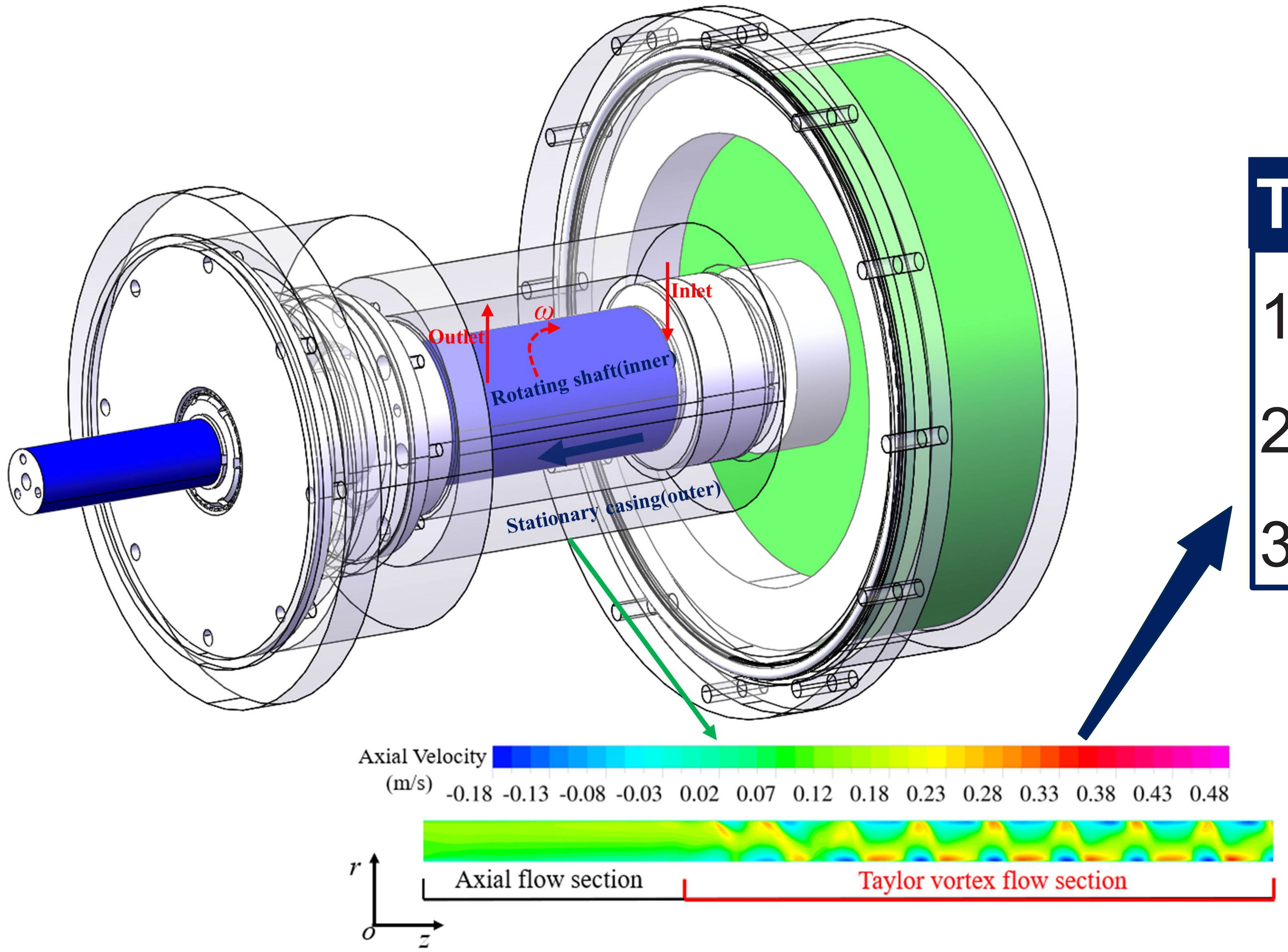

Taylor vortices

1. Temperature fluctuations
2. Pressure fluctuations
3. Wind friction losses

INTRODUCTION

◆ Research purposes

— Study the flow characteristics / initial position of Taylor vortices (Predictive model)

— Find measures to weaken fluctuations and reduce excitation

◆ Supercritical carbon dioxide Taylor-Couette-Poiseuille flow

1. sCO_2 has high density and low viscosity
2. Turbine shafts run at exceptionally high speeds

Ta:1×10^{12} ~

Re_a:1×10^{5} ~

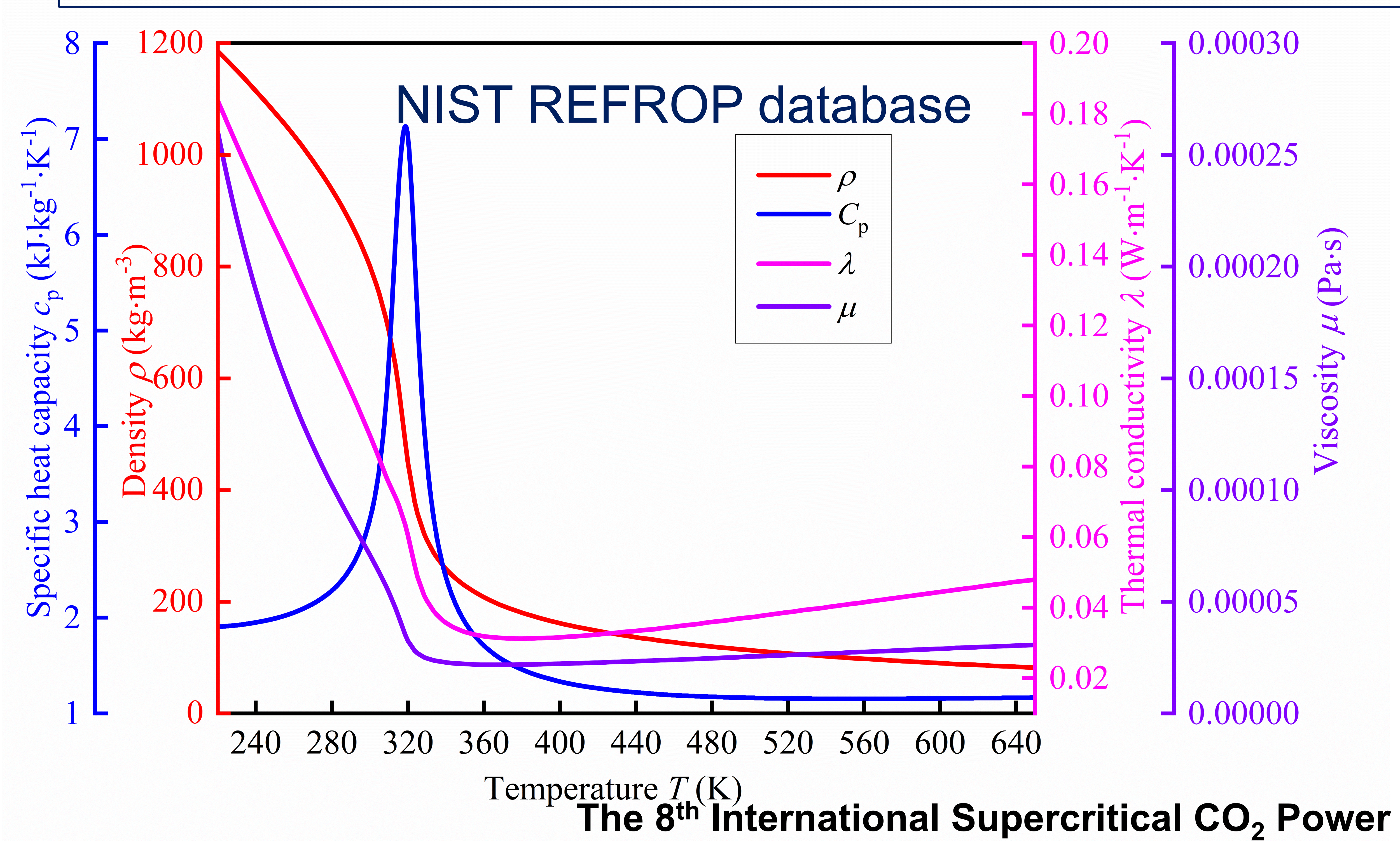

Taylor-Couette-Poiseuille flow physical model

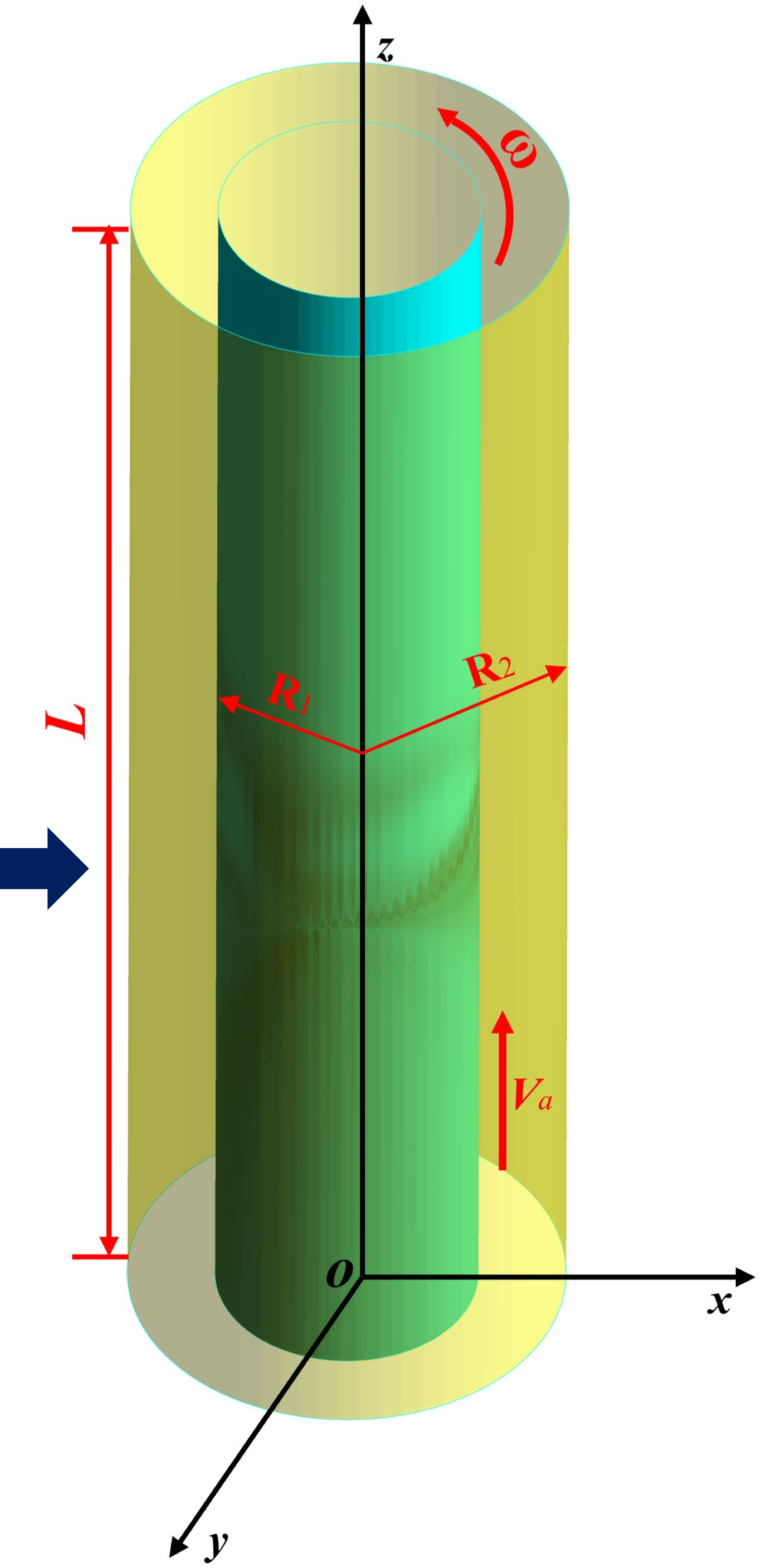

RESEARCH METHODS

◆ Research literature review of Supercritical carbon dioxide Taylor vortex

1. Heat transfer
2. Resistance loss

✓

Under high Re_a and Ta conditions, the initial position of Taylor vortices formed by sCO_2, along with the methods to suppress their formation, have not been fully elucidated.

◆ Research methods

1. Experimental

   — Experimental conditions are strict, difficult to observe Taylor vortices

   — Flow field parameters are difficult to accurately measure

2. **CFD method** ✓

   — Accurate calculation of flow field parameters

   — Conduct large-scale parameter studies

3. **Matrix nonlinear regression/Neural Networks** ✓

   — Powerful high-dimensional data processing and non-linear relationship capture capabilities

PHYSICAL MODEL

- **Computational model**

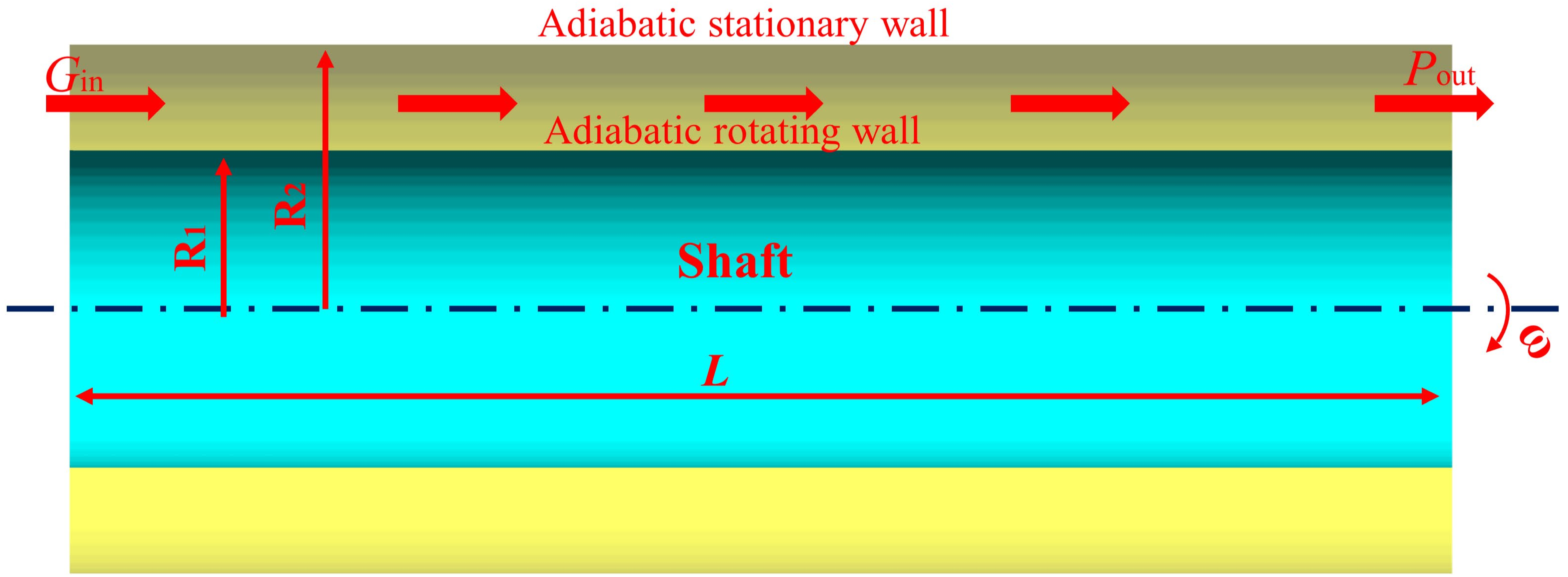

- **Key parameter**

Radius ratio $\eta = (R_2 - R_1)/R_1$

Gap width $\delta = R_2 - R_1$

Aspect ratio $\Gamma = L/\delta$

Reynolds number $Re_a = \dfrac{V_a D_h}{\nu}$

Taylor number $Ta = \dfrac{\omega^2 R_1 (D_h/2)^3}{\nu^2}$

- **Meshing**

1. Structured mesh
2. Encryption of inner and outer walls

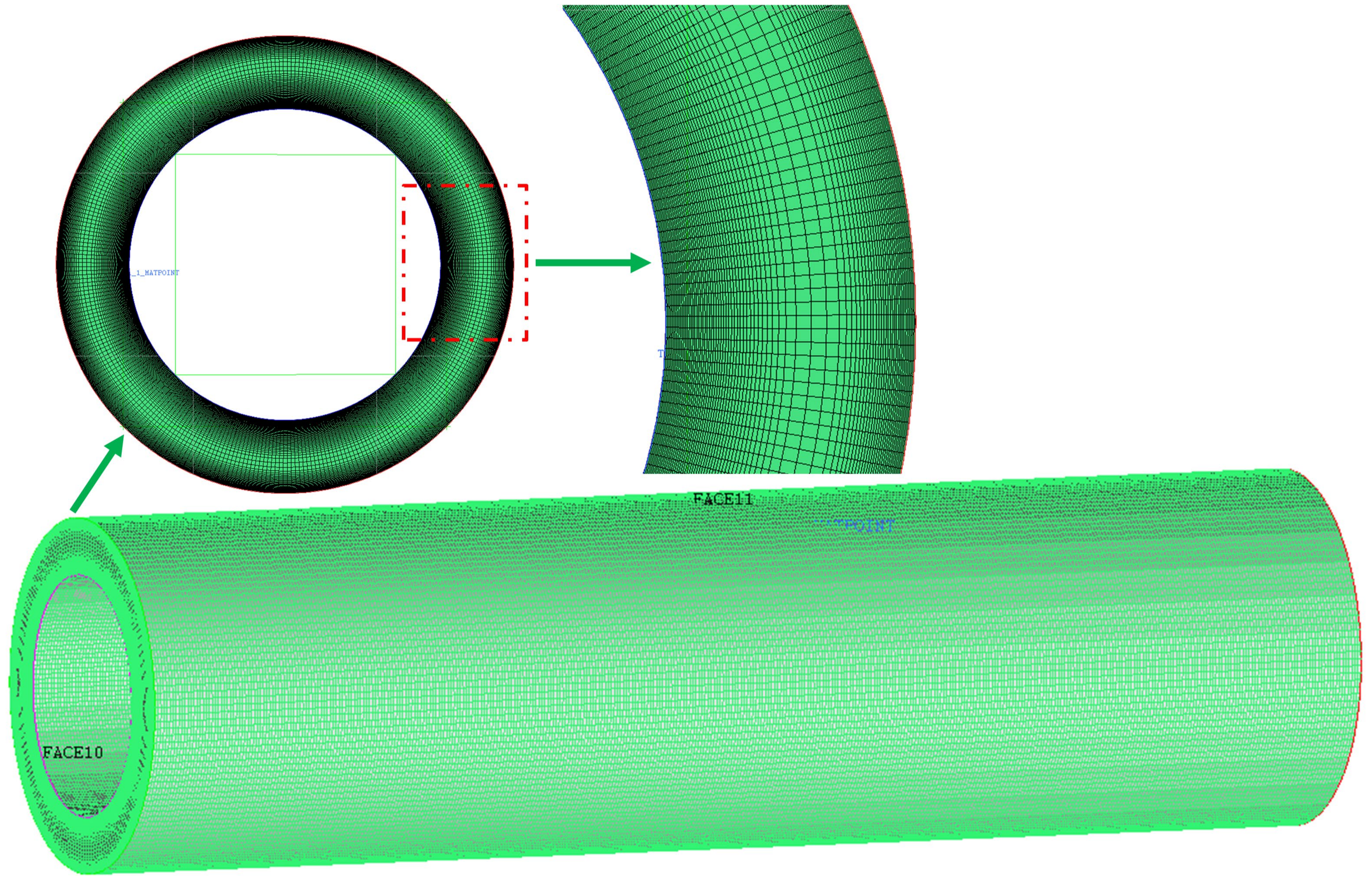

- **Physical properties parameters**

NIST REFORP physical properties database

GRID INDEPENDENCE VERIFICATION

◆ Grid independence verification

Model parameters and simulation conditions

Parameter	Value
R_1	12.5mm
Annulus height	4mm
L	136mm
ω	0~25000RPM
T_s	50~150℃
sCO_2 temperature	50℃
sCO_2 pressure	10MPa
sCO_2 Mass Flow	0.015kg/s~0.24kg/s

Nu simulation results at different grid numbers

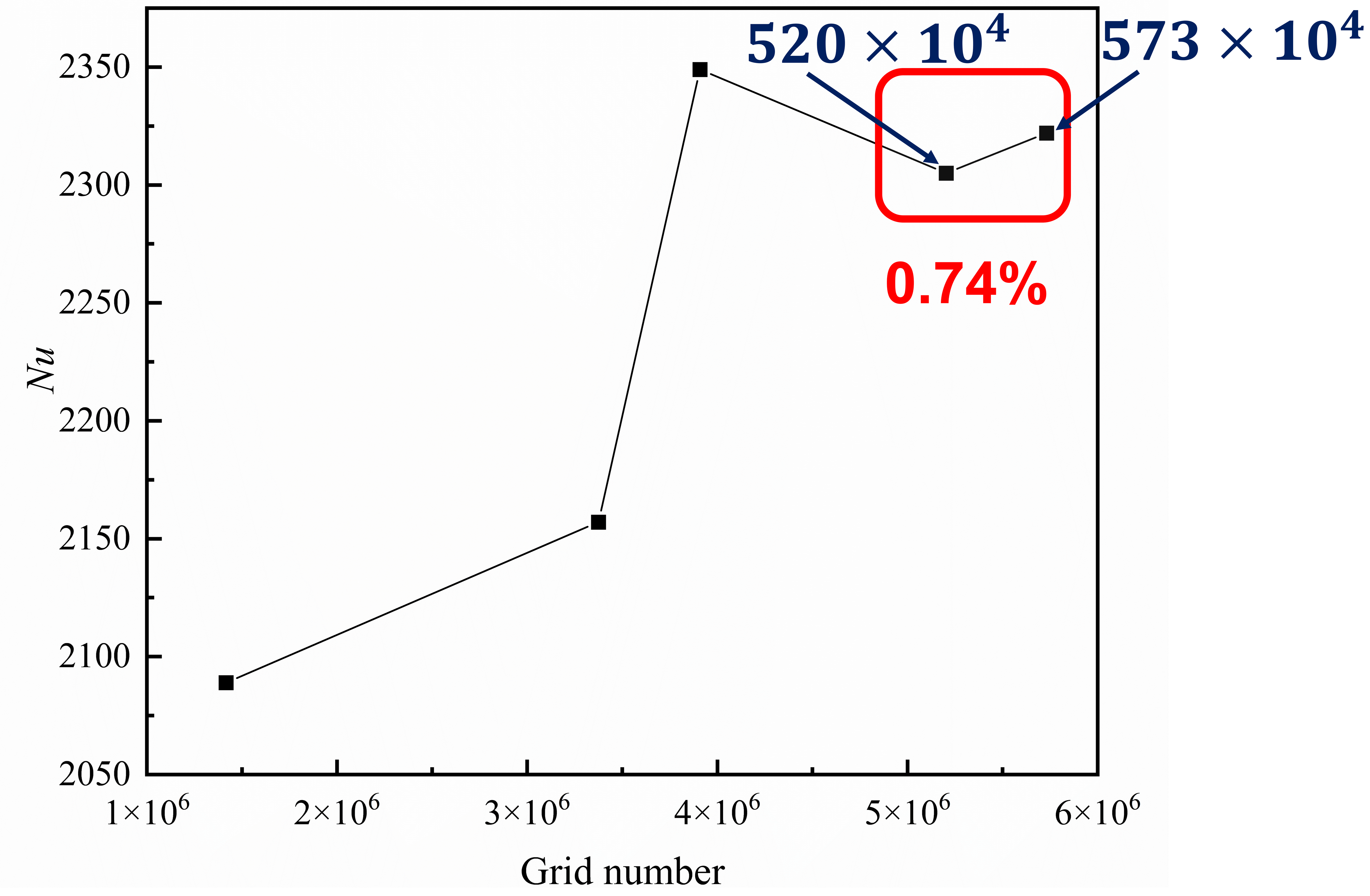

1. As the number of grids increases, the variation in Nu values among different grid numbers gradually diminishes.
2. The number of grids is 573×10^4.

ALGORITHM RELIABILITY VERIFICATION

◆ **Numerical simulation algorithm reliability verification**

Nu calculation formula (From Swann et al.)

$$Nu = 8.2 \times 10^{-3} Re_{eff}^{0.84}$$

$$Re_{eff} = \frac{\sqrt{V_a^2 + V_w^2}\rho D_h}{\mu}$$

Model parameters and simulation conditions

Parameter	Value
R_1	12.5mm
Annulus height	4mm
L	136mm
ω	0~25000RPM
T_s	50~150℃
$_sCO_2$ temperature	50℃
$_sCO_2$ pressure	10MPa
$_sCO_2$ Mass Flow	0.015kg/s~0.24kg/s

Comparison of simulation results and calculation results

T_s /K	Formula (6) Calculated	k-ω SST		k-ω Standard		k-ε RNG		k-ε Realizable	
		Simulation	error %	Simulation	error %	Simulation	error %	Simulation	error %
343.15	2418.13	2322.37	-3.96	2245.05	-7.16	2209.76	-8.62	2330.21	-3.64
353.15	2201.70	2249.60	2.18	2157.27	-2.02	2124.85	-3.49	2129.23	-3.29

RESULTS AND DISCUSSION

◆ Characteristics of Taylor Vortex formed by sCO_2

Rotation speed 200rad/s

Mass flow rate 0.008kg/s

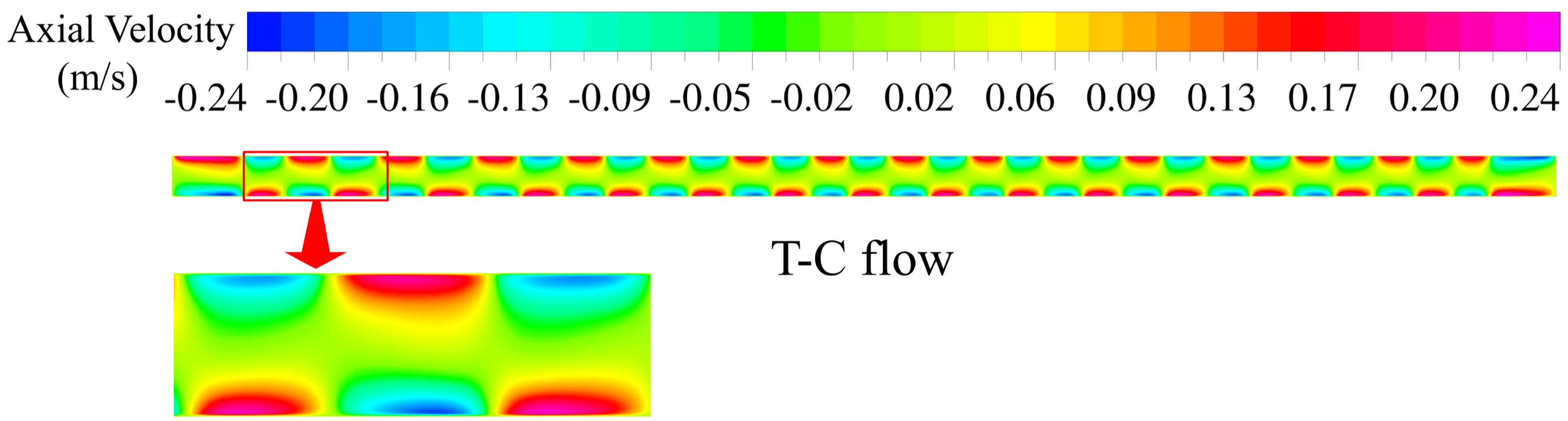

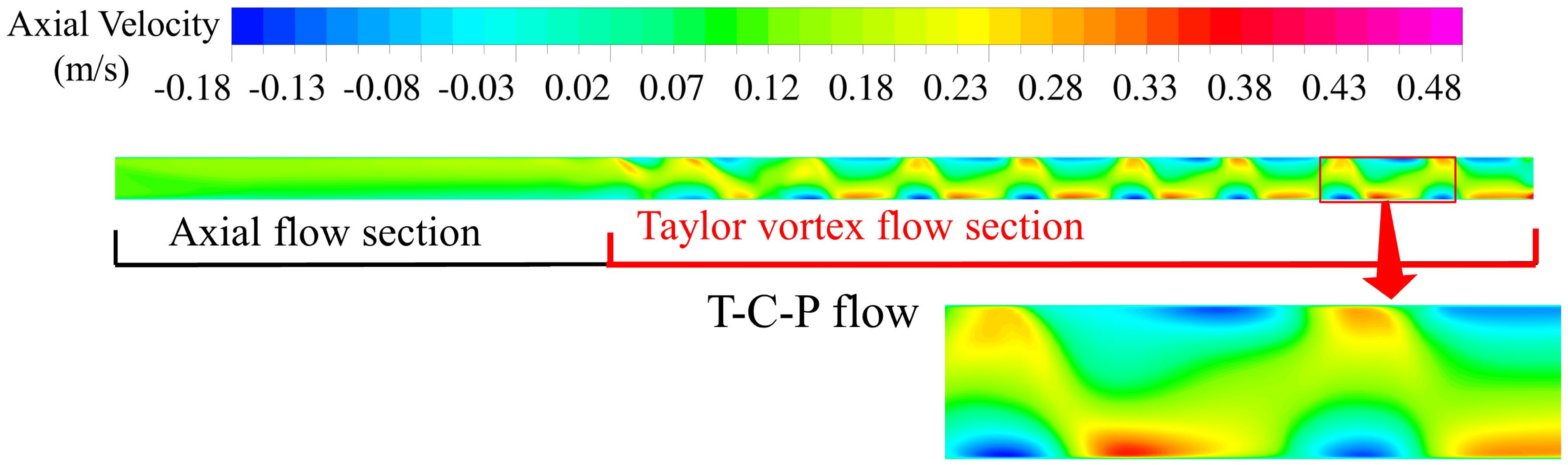

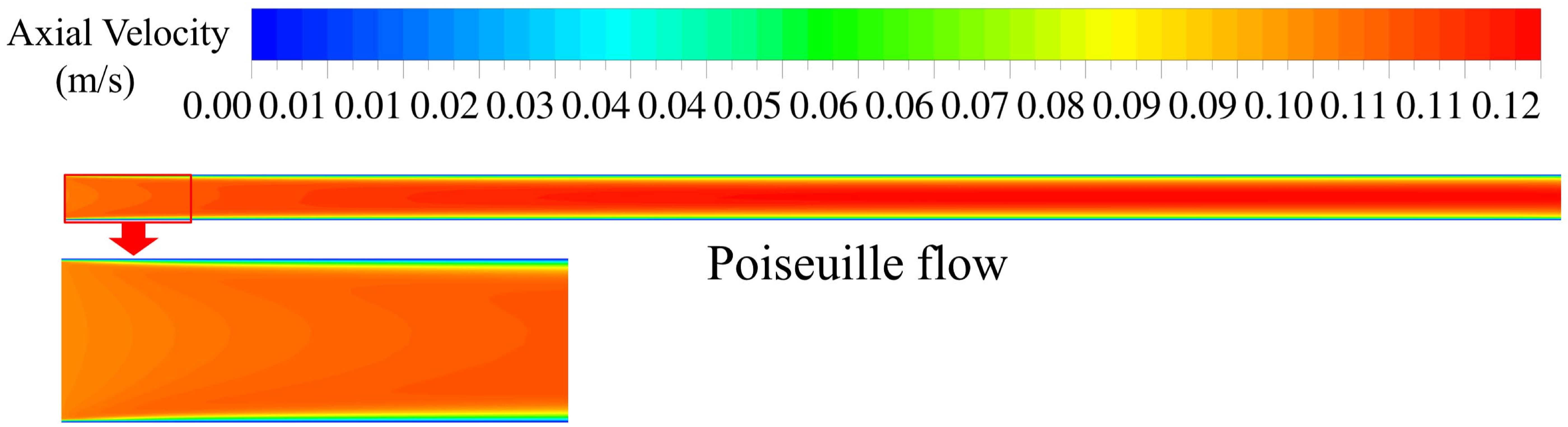

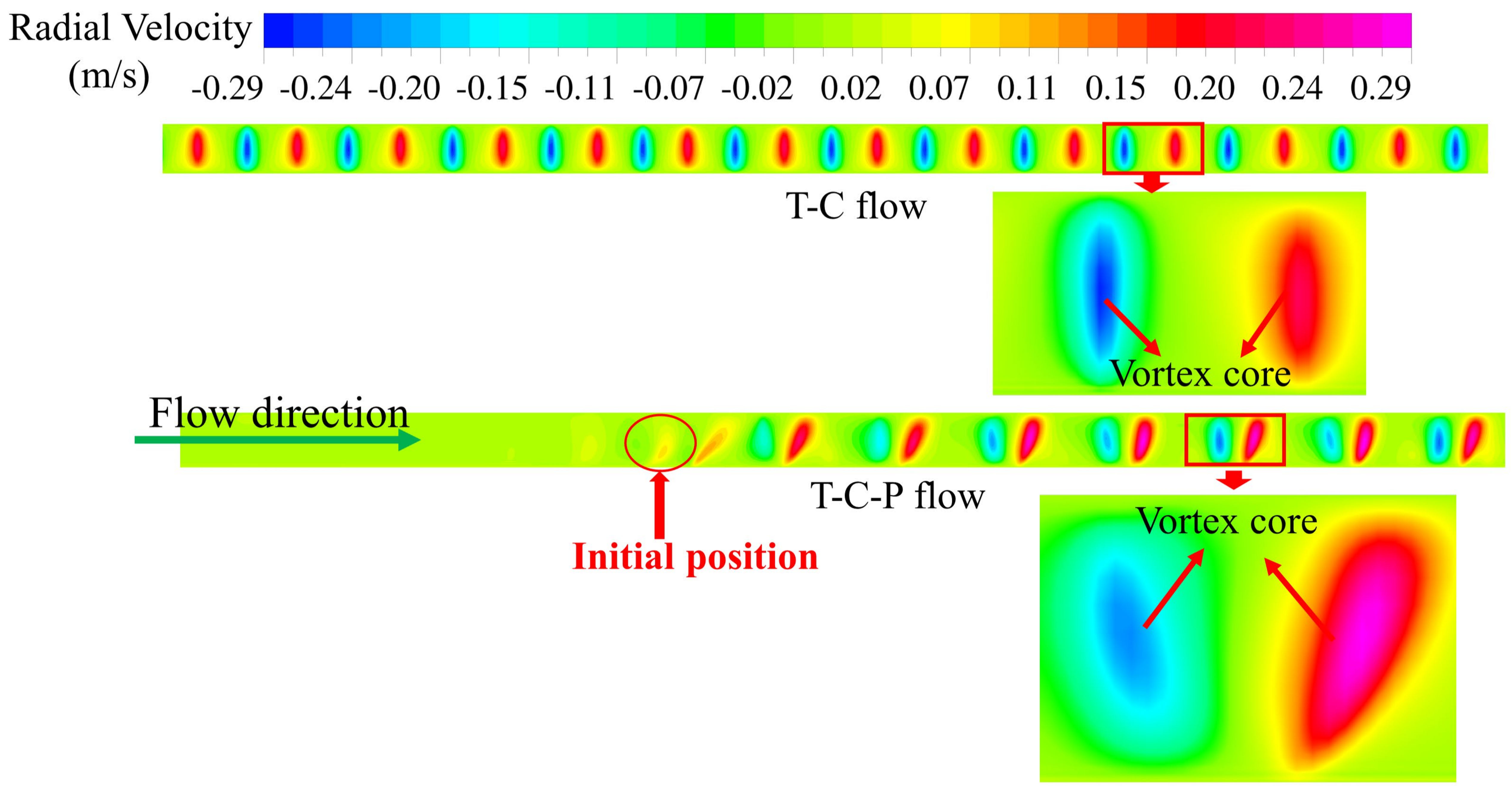

RESULTS AND DISCUSSION

◆ **Taylor vortex initial position contours**

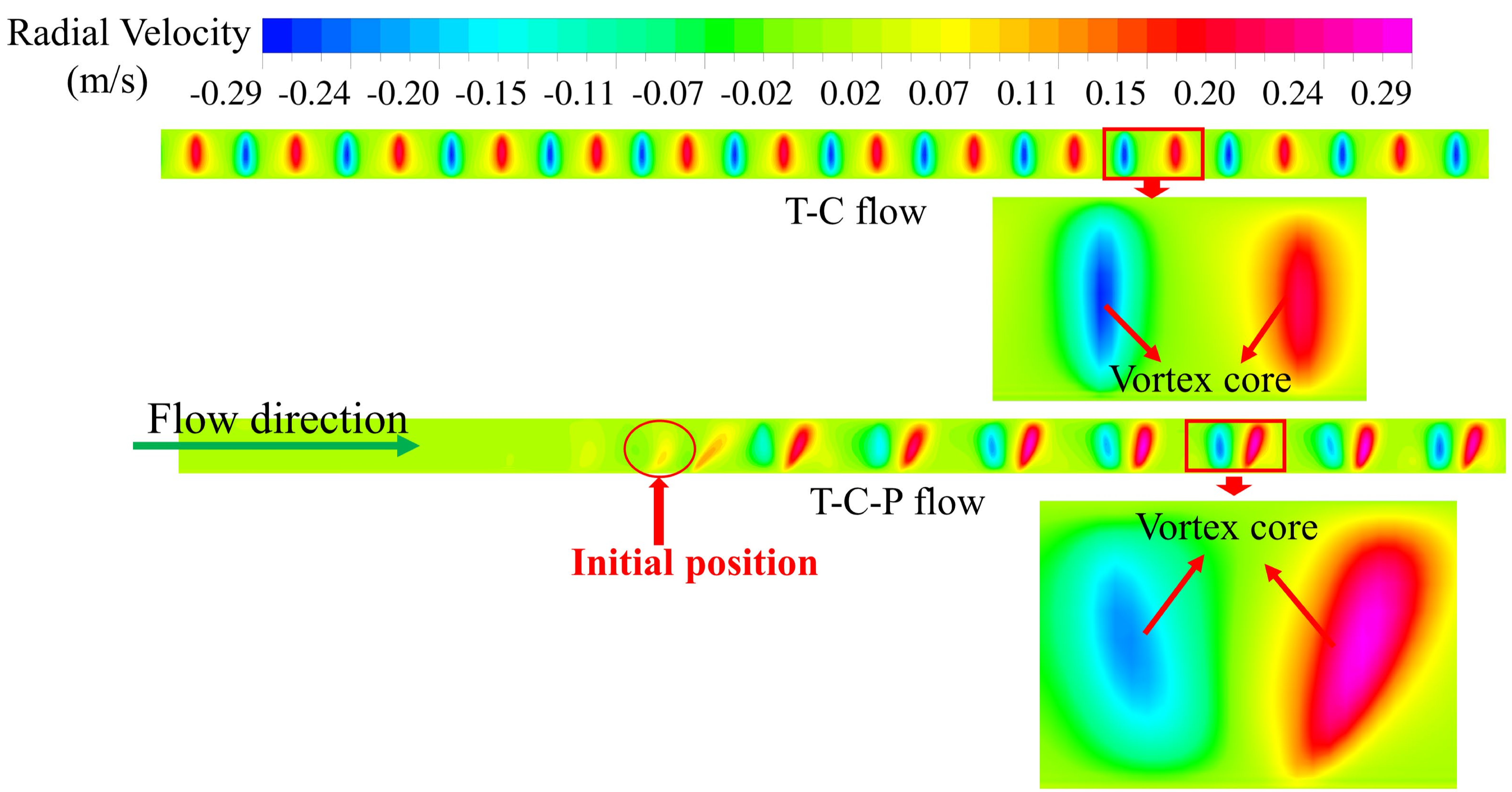

◆ **Taylor vortex radial velocity profile**

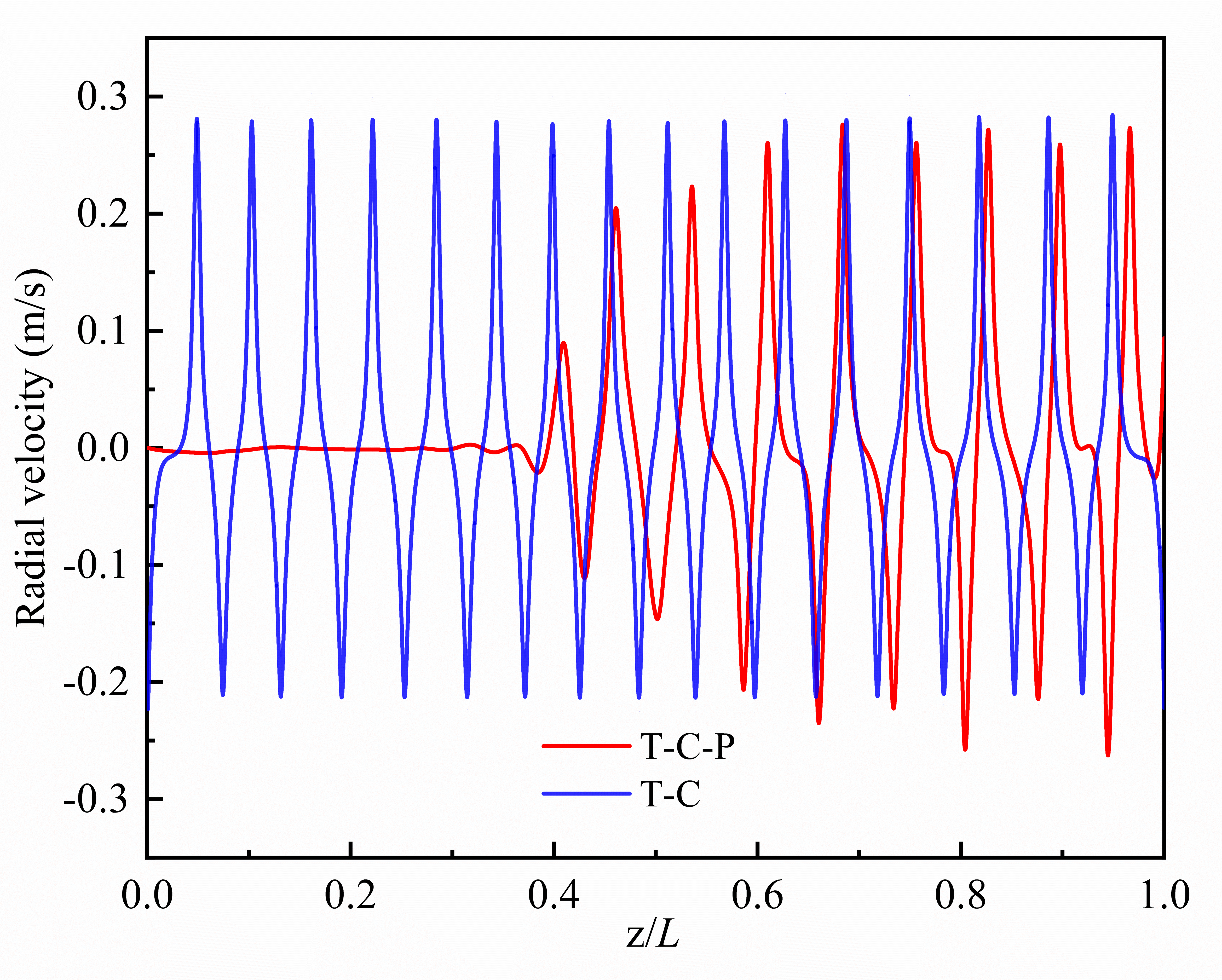

1. When unsteady secondary flow occurs, the starting position of the Taylor vortex, where the first vortex appears, is its **initial position.**
2. The radial velocity profile shows a periodic change of positive and negative alternations.

RESULTS AND DISCUSSION

◆ **Detailed parameter setting**

Simulate working conditions	1	2	3	4
Inner wall radius	12.5mm			
Inlet temperature	110℃			
Pressure	10MPa			
Axial Reynolds number	$\mathbf{6.6 \times 10^{3} \sim 2.0 \times 10^{5}}$	9.6×10^{4}	$3.0 \times 10^{4} \sim 2.0 \times 10^{5}$	9.6×10^{4}
Taylor number	5.48×10^{11}	$\mathbf{0 \sim 1.52 \times 10^{12}}$	$3.3 \times 10^{10} \sim 6.24 \times 10^{12}$	7.04×10^{11}
Radius ratio	0.32	0.319	**0.11~0.67**	0.32
Aspect ratio	34	34	16~108	**16~99**

The radius of the rotating wall, the inlet temperature of sCO_2, and the working pressure remain constant.

RESULTS AND DISCUSSION

1. The effect Re_a on the initial position of the Taylor vortex

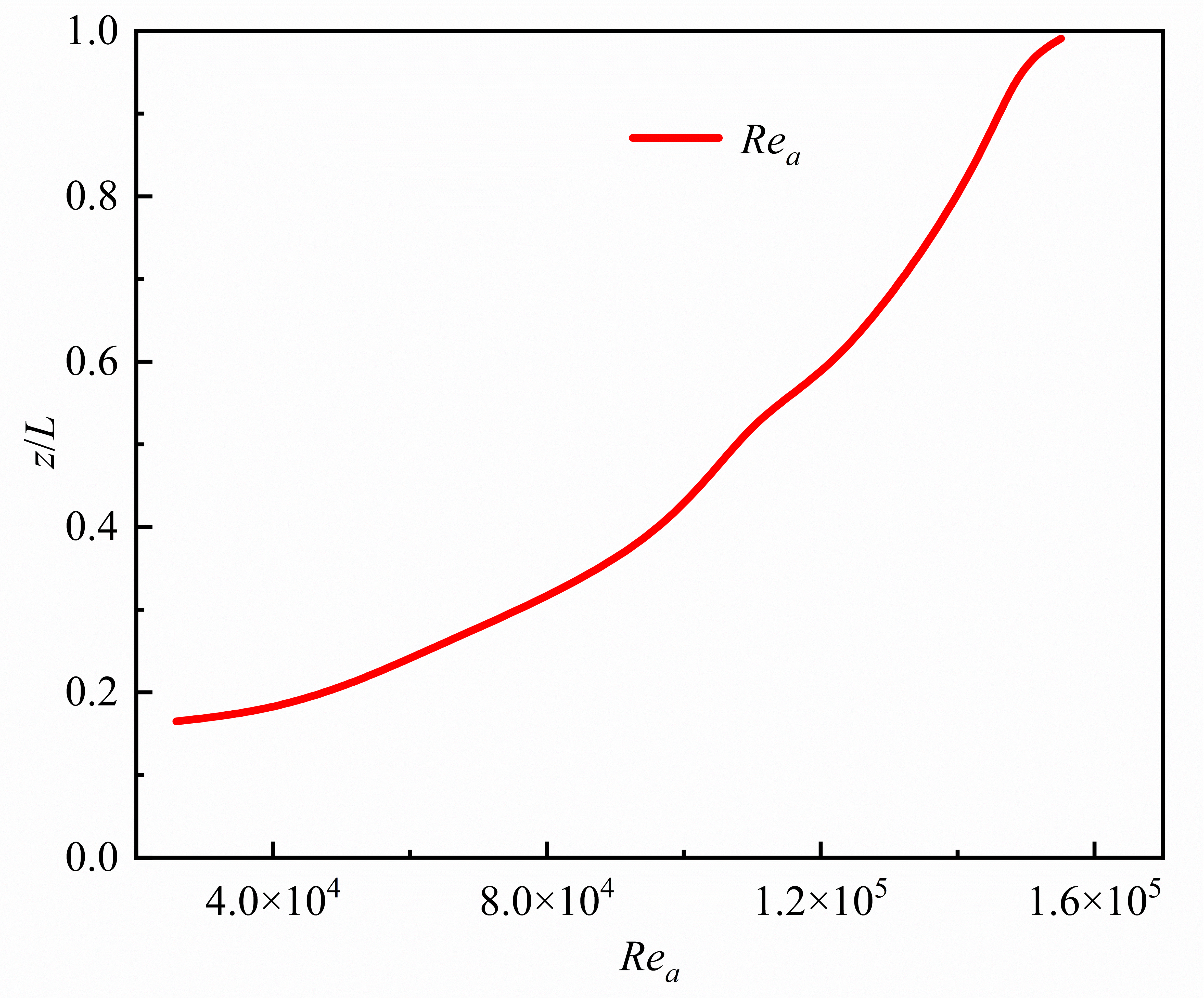

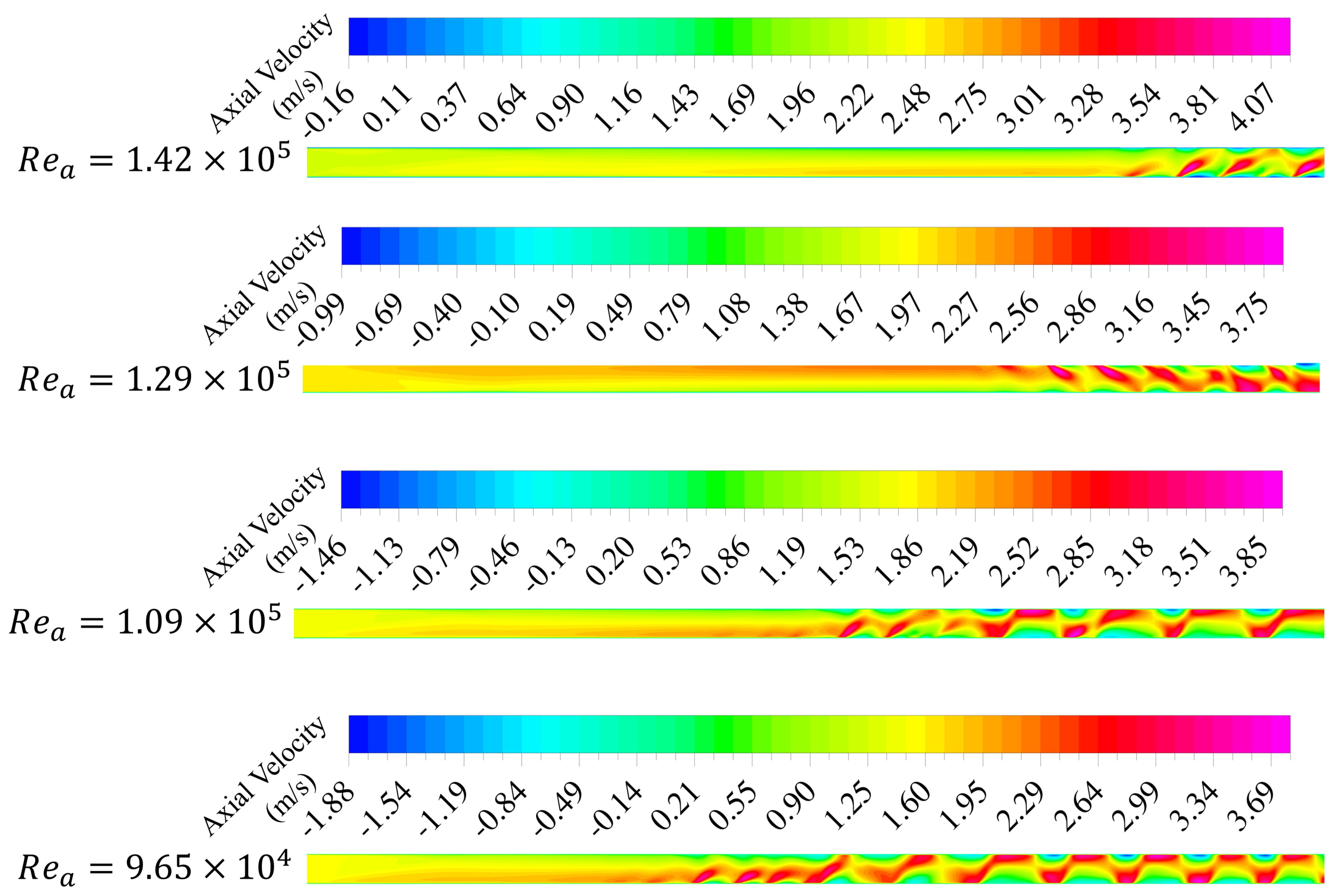

Boosting the inlet flow rate of the T-C-P flow can enhance the stability of the flow and effectively inhibit the formation of Taylor vortices.

2. The effect of Ta on the initial position of the Taylor vortex

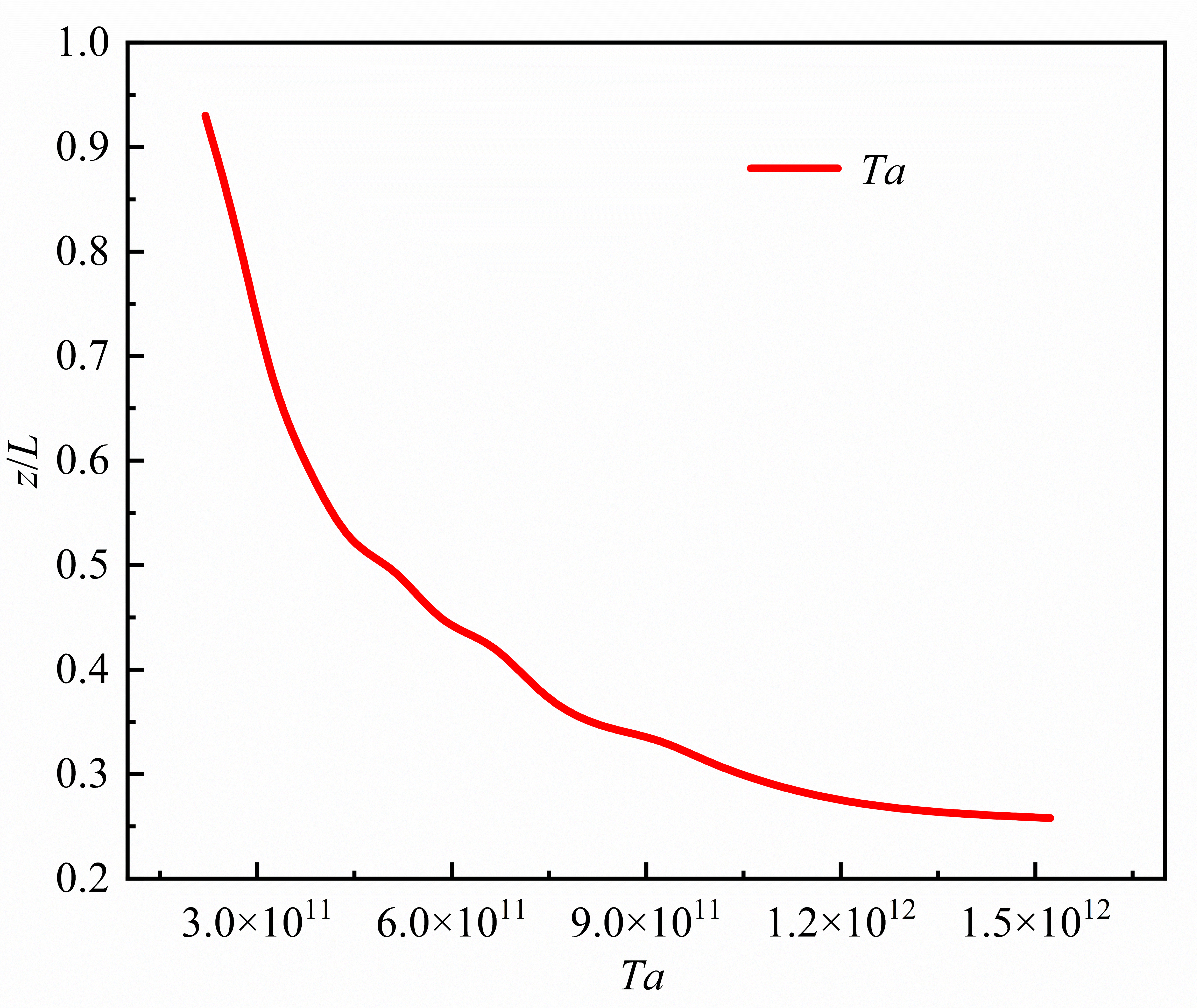

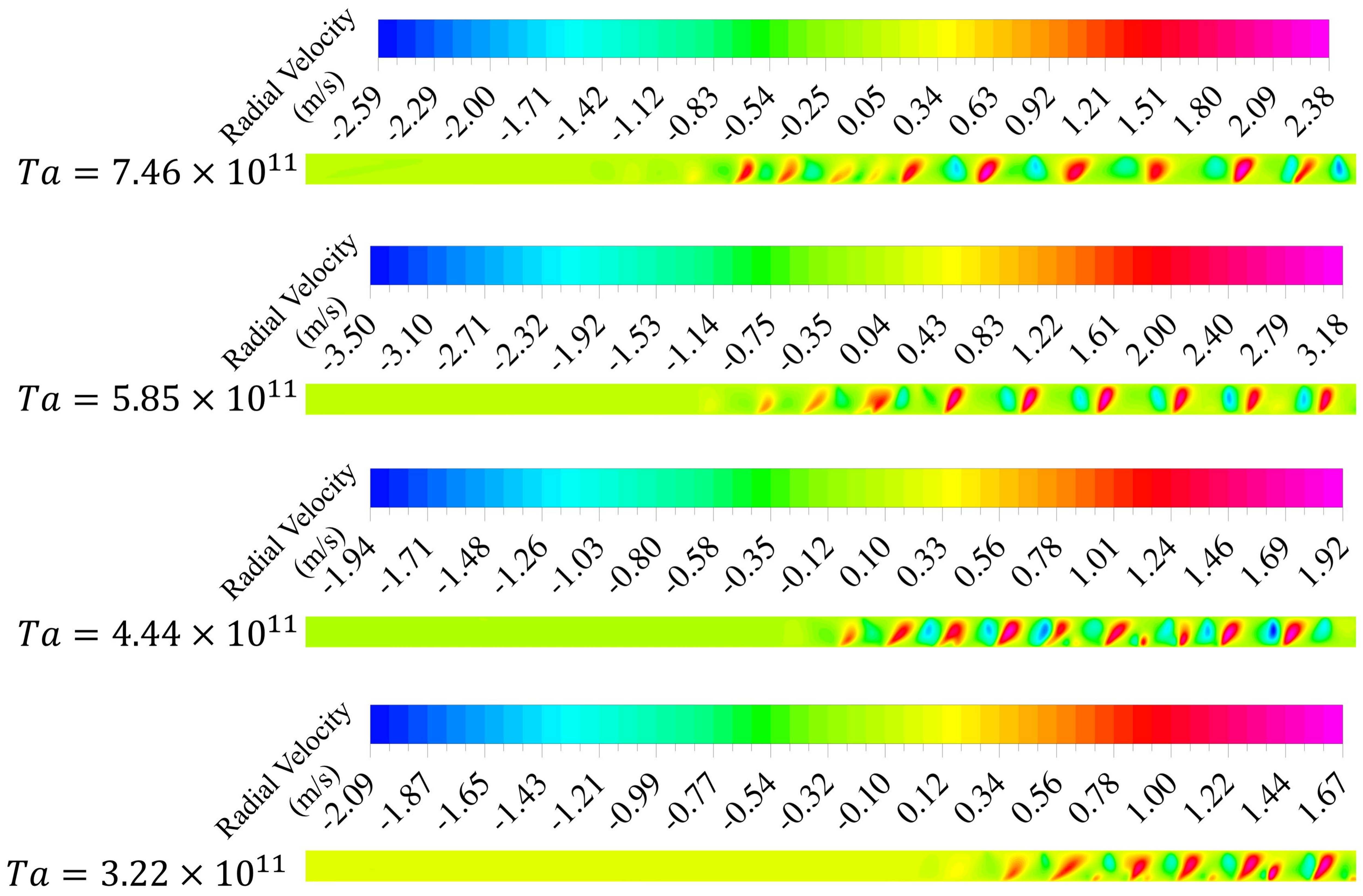

Elevating the rotational speed results in heightened instability for the T-C-P flow, an augmented quantity of Taylor vortices, and a closer proximity of the initial position of the Taylor vortex to the inlet.

3. The effect of *η* on the initial position of the Taylor vortex

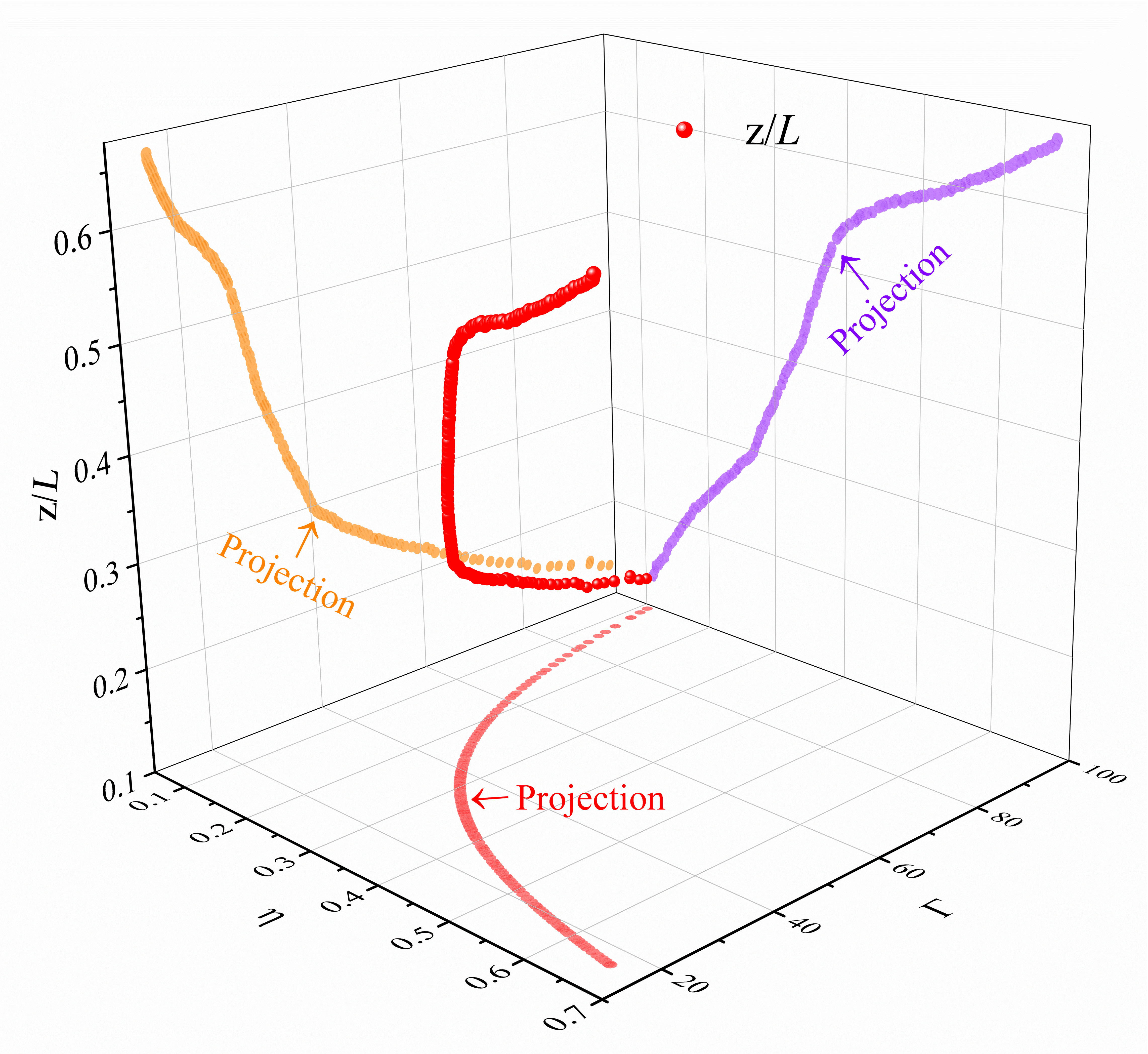

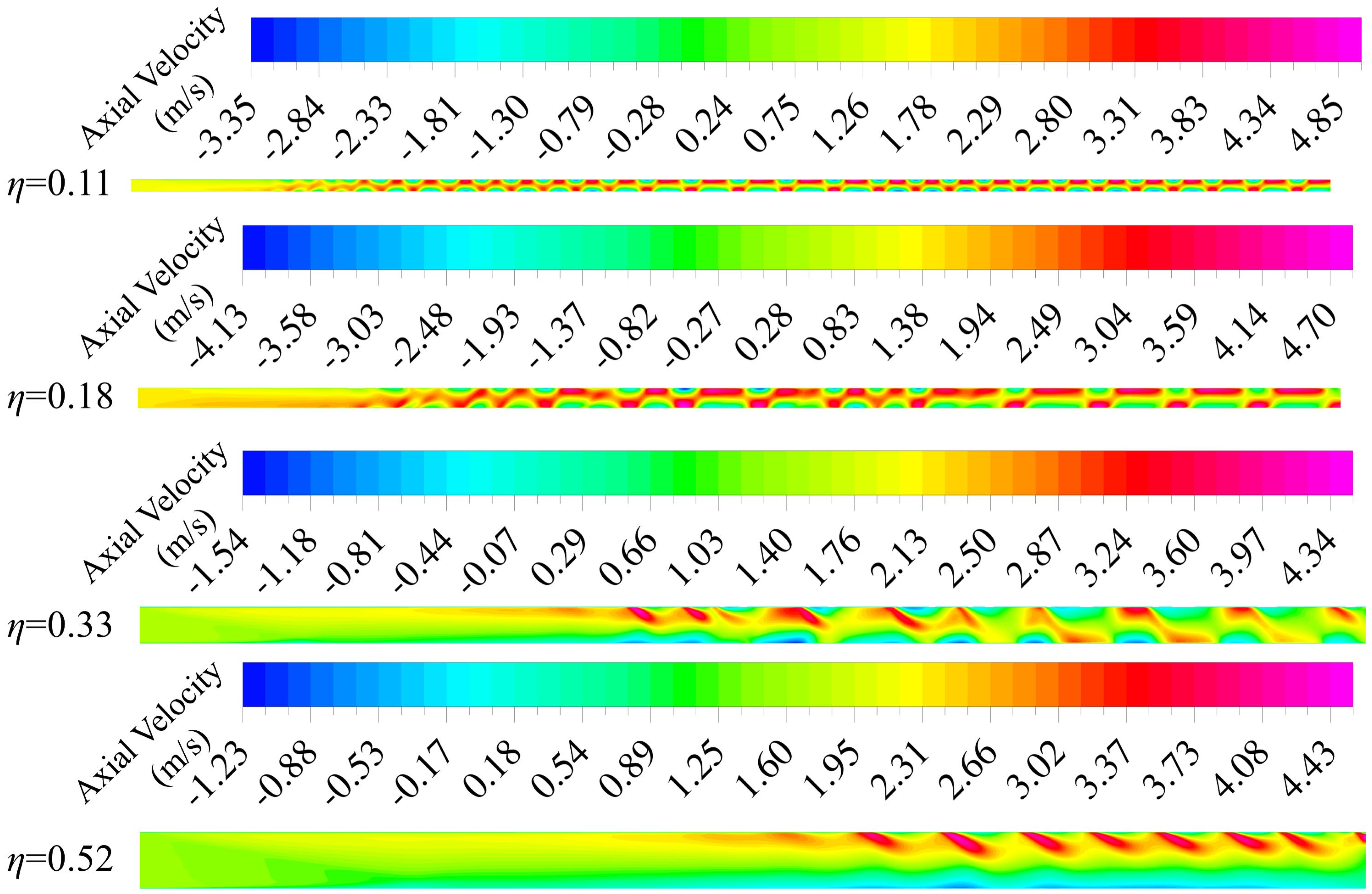

Keeping the streamwise length of the T-C-P flow constant while maintaining the same axial flow velocity and rotational speed, increasing *η* will effectively suppress the formation of Taylor vortices.

RESULTS AND DISCUSSION

4. The effect of Γ on the initial position of the Taylor vortex

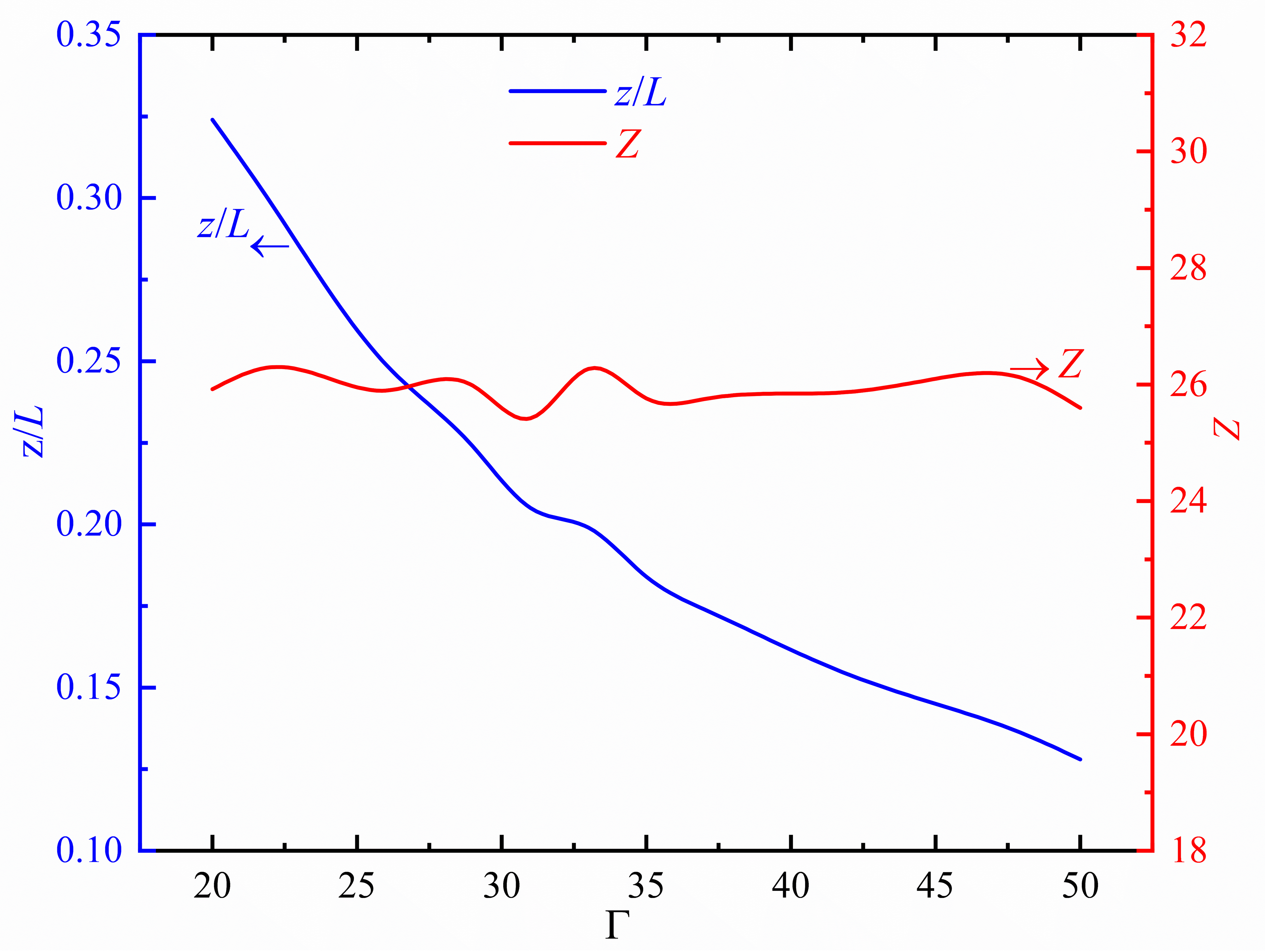

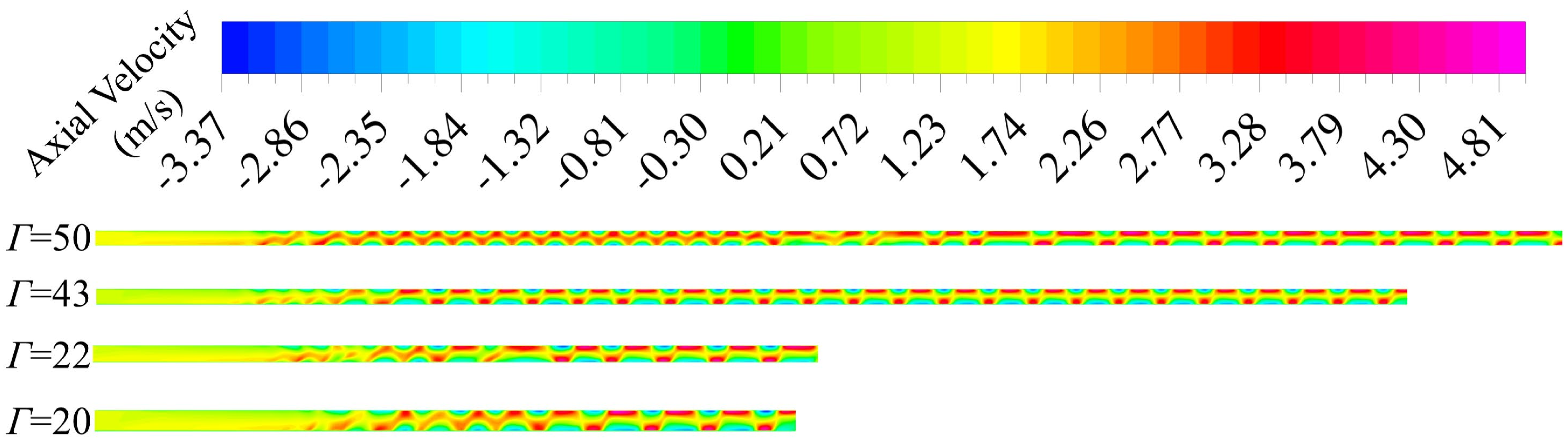

As Γ increases, the initial relative position z/L of the Taylor vortex diminishes progressively.

The absolute location Z of the Taylor vortex remains virtually constant.

RESULTS AND DISCUSSION

◆ Multivariate matrix exponential regression model construction

$$z/L=A\left(\frac{V_a D_h}{\nu}\right)^{x_1}\left(\frac{\omega^2 R_1 (D_h/2)}{\nu^2}\right)^{x_2}\left(\frac{R_2-R_1}{R_1}\right)^{x_3}\left(\frac{L}{R_2-R_1}\right)^{x_4}$$

$$\ln A\cdot\ln e+x_1\ln\left(\left(\frac{V_a D_h}{\nu}\right)_{n1}\right)+x_2\ln\left(\left(\frac{\omega^2 R_1(D_h/2)}{\nu^2}\right)_{n2}\right)+x_3\ln\left(\left(\frac{R_2-R_1}{R_1}\right)_{n3}\right)+x_4\ln\left(\left(\frac{L}{R_2-R_1}\right)_{n4}\right)=\ln((z/L)_n)$$

$$B=\begin{pmatrix}\ln e & \cdots & \ln\left(\frac{L}{R_2-R_1}\right)_{14}\\ \vdots & \ddots & \vdots \\ \ln e & \cdots & \ln\left(\frac{L}{R_2-R_1}\right)_{n4}\end{pmatrix}\qquad X=\begin{pmatrix}\ln A\\ x_1\\ x_2\\ x_3\\ x_4\end{pmatrix}\qquad Y=\begin{pmatrix}\ln(z/L)_{11}\\ \ln(z/L)_{21}\\ \ln(z/L)_{31}\\ \vdots\\ \ln(z/L)_{n1}\end{pmatrix}$$

$$z/L=3.1934\times10^6\left(\frac{V_a D_h}{\nu}\right)^{0.5651}\left(\frac{\omega^2 R_1(D_h/2)}{\nu^2}\right)^{-0.7488}\left(\frac{R_2-R_1}{R_1}\right)^{-0.3821}\left(\frac{L}{R_2-R_1}\right)^{-0.7400}$$

1. Suppressing the generation of Taylor vortices in the turbine shaft can be achieved by increasing the inlet flow rate, reducing the shaft speed.
2. Approximate solution. Not suitable for large-scale and high-precision prediction.

RESULTS AND DISCUSSION

◆ Neural network model

Network model structure diagram

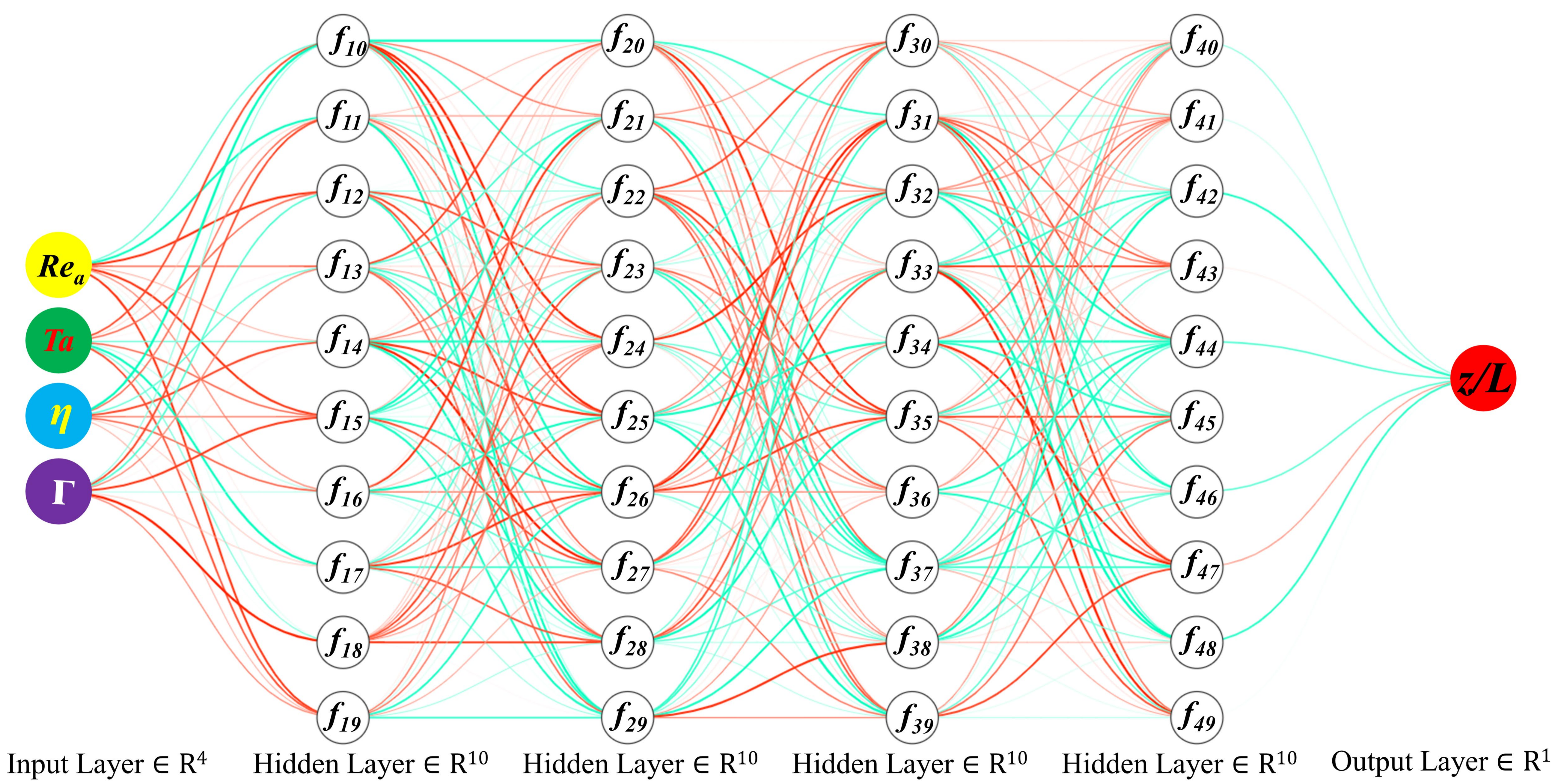

◆ Model parameter settings

Parameter	Set up
neural network model	feedforward backpropagation
number of iterations	10000
performance value	0.0001
learning rate	0.001
algorithm function	Levenberg-Marquardt
transfer function	Tansig-Purelin
performance function	MSE

◆ Data transfer

560 sets of data, 70% of the data is selected as the training set, 15% of the data is the verification set, and 15% of the data is the test set.

◆ Neural network model calculation results

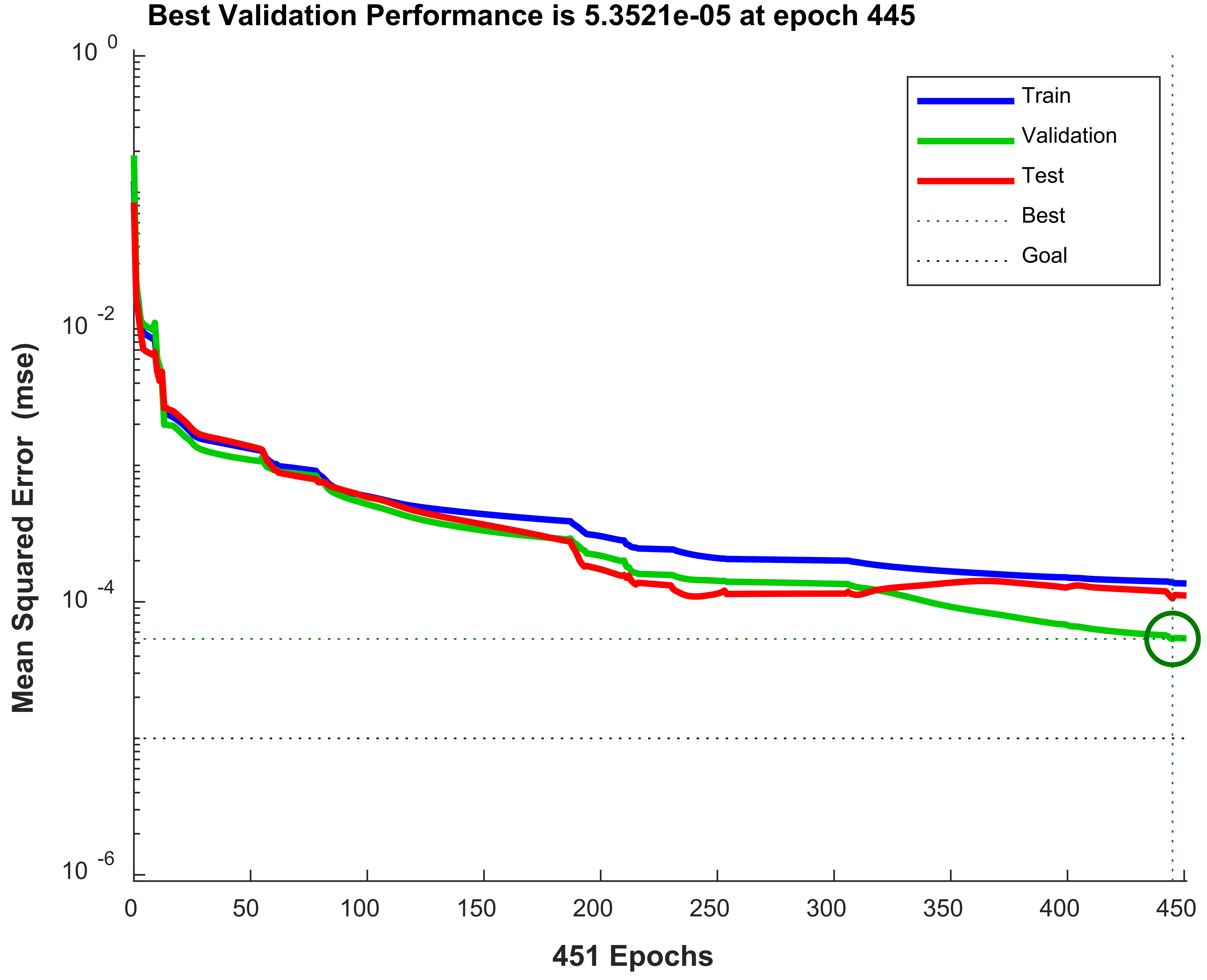

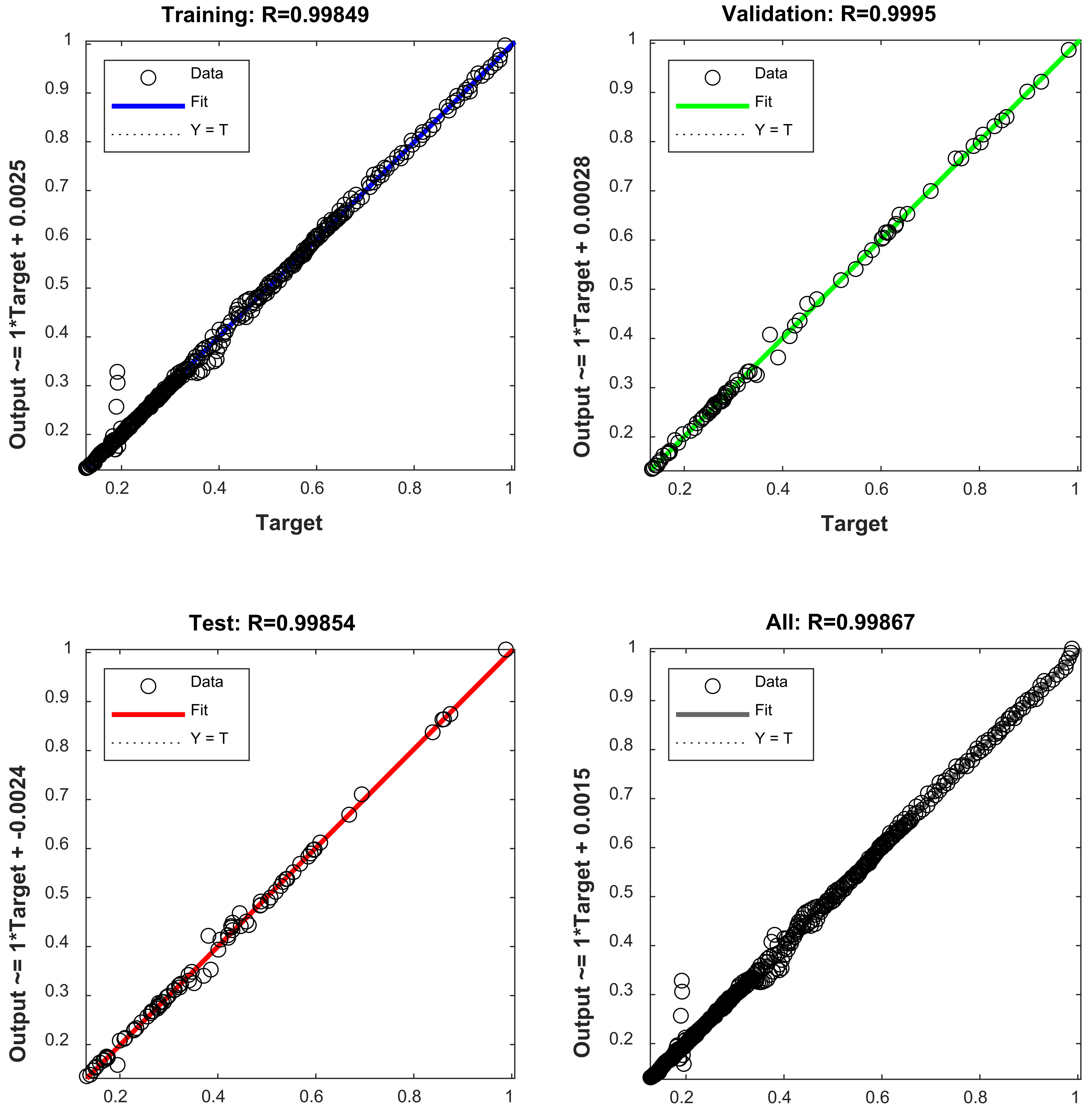

1. Most of the data points align closely with the fitted data line.
2. The 4-10-1 Taylor vortex initial position prediction model can achieve precise forecasts.

RESULTS AND DISCUSSION

◆ **Comparison between matrix nonlinear regression and neural network**

Parameter settings

Parameter	Value
R_1	12.5mm
R_2	16.5mm
T_{in}	110℃
P	10MPa
ω	14000RPM~50000RPM
η	0.11~0.66
r	16~99

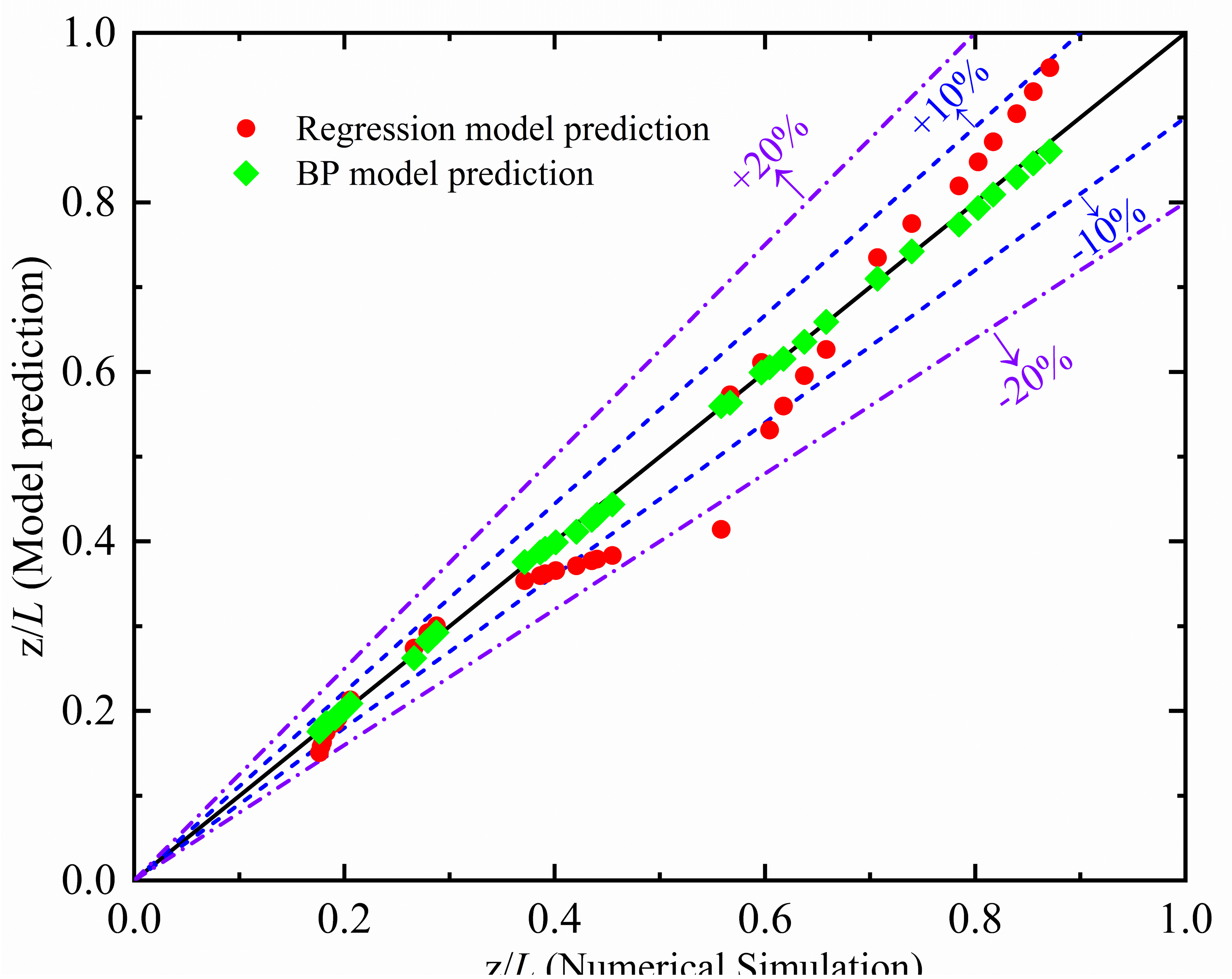

1. The forecasted values from the neural network model align with the simulated values, with error margins staying below 10%.
2. With the exception of the interval between 0.2 and 0.4, the predicted values for the initial positions in the remaining position regression models diverge significantly from the simulated values.

The most accurate model for predicting the initial position is the established 4-10-1 neural network model.

CONCLUSIONS

1. sCO_2 forms a Taylor-Couette-Poiseuille flow within the clearance between the turbine shaft and the stationary casing. The T-C-P flow includes a stable flow section and a Taylor vortex section. The Taylor vortex distribution formed by the T-C-P flow presents as a structurally oblique vortex.
2. The generation of Taylor vortex in the sCO_2 turbine shaft can be suppressed and the flow stability of sCO_2 in the turbine shaft can be improved by increasing the flow rate, reducing the rotational speed, increasing the radius ratio and reducing the aspect ratio.
3. The prediction accuracy of the matrix nonlinear regression model is lower when compared to the 4-10-1 feedforward neural network model. Specifically, the 4-10-1 feedforward neural network model achieves a prediction accuracy within 10% for the initial position.

ACKNOWLEDGMENTS

1. The National Natural Science Foundation of China (Grant No.52176090).
2. The Youth Team Support Plan in Basic Research of the Chinese Academy of Sciences (Grant No.YSBR-043).
3. The Major national science and technology infrastructure “High-Efficiency and Low-Carbon Gas Turbine Research Facility” (2017-000052-73-01-001569).

◆The **Major National Science and Technology Infrastructure Project of China**

High-Efficiency and Low-Carbon Gas Turbine Research Facility (HiGT)

Supercritical CO_2 power cycle test rig

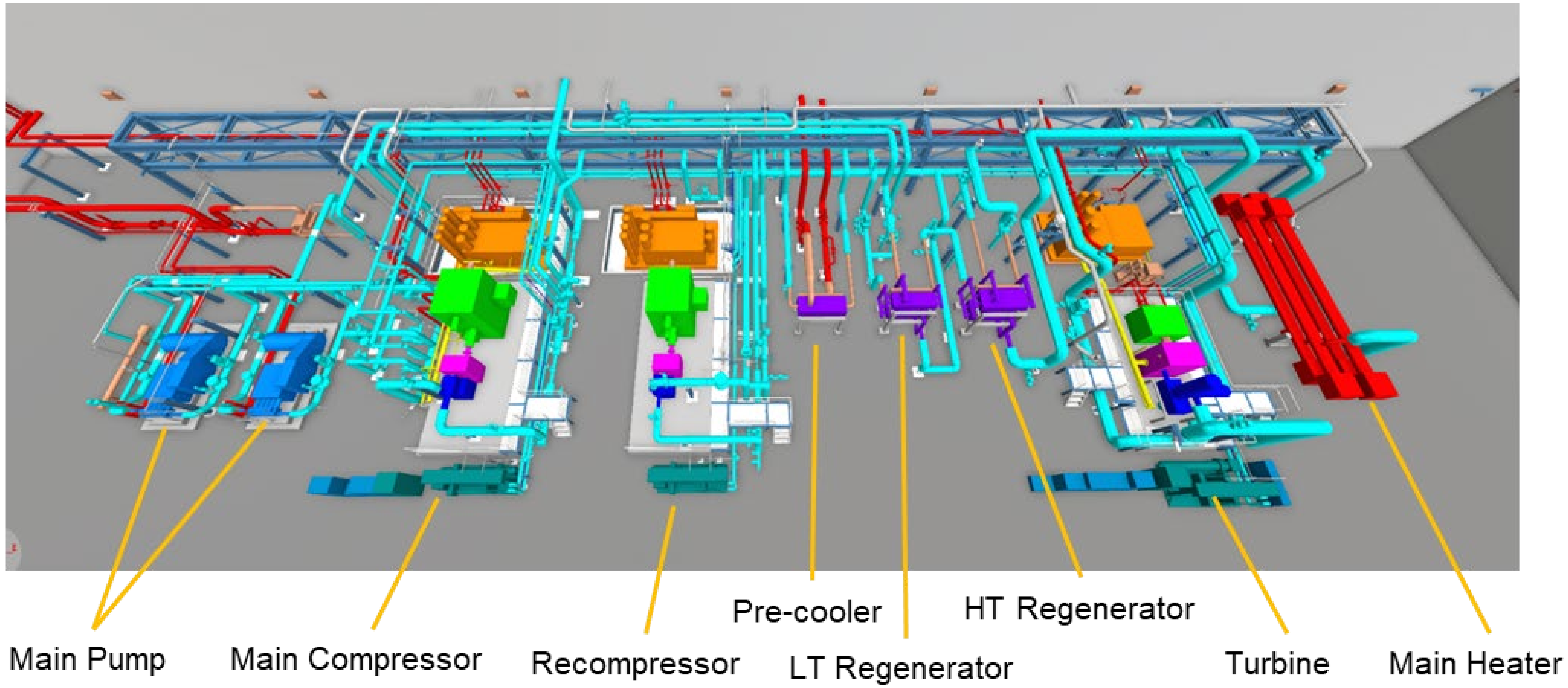

Cycle parameters

Max P&T: 24MPa, 600°C

Mass flow: 8~35kg/s

Max Output power: 3MWe

Max Heater power: 8MWt

Rig capability

Component testing

Compressor&pump

Turbine

Heat exchanger

Cycle testing

System performance & dynamics

Loop optimization

INFRASTRUCTURE PROJECT

◆ The HiGT-SCO_2 Test Bench Status Update

The test bench is expected to be put into operation in September 2024.


View of test bench construction in the plant(Shanghai)


Compressor


Turbine


Electric heater


Regenerators

With the principle of full openness and sharing, all scholars and institutions are welcome to visit and cooperate on this test rig.

◆**International Conference on Supercritical carbon dioxide Power Cycle and Comprehensive Energy Systems**

◆September 20-24, **2024 Shanghai, China**

Topics

Thermodynamics & System Integration of Supercritical Power Cycle	Supercritical Fluid Flow **Heat Transfer** & Heat Exchanger
Supercritical Fluid Thermal Power Conversion & **Equipment**	Supercritical Composite Fluid Power Cycle
Supercritical Fluid **Energy Storage**/CCUS Theory and Technology	Supercritical Fluid Chemical & **Materials** Technology
...	

Timelines

Apr 30 , 2024 Abstract submission
May 15, 2024 Abstract acceptance notification
Jun 15, 2024 Full paper submission
Jul 15, 2024 Notification of full paper acceptance
Aug 15, 2024 Early Bird Registration

Please contact:

Miss Li：010-82543109/18811727608 （Meeting Affairs）, IET, CAS, China

Email: ICSPC2023@163.com

Thank You for your attention!

Question

- Contact us: guochaohong@iet.cn
  lufengxiong@iet.cn